IAEA-F4-TM-42581

Recent Progress on Tungsten Spectroscopy And Its Data Analysis in Large Helical Device

S.Morita[a,b], T.Oishi[a], I.Murakami[a,b], M.Goto[a,b], X.L.Huang[b], D.Kato[a,b], H.A.Sakaue[a], H.M.Zhang[b], K.Fujii[c], M.Hasuo[c], L.Q.Hu[d], Z.W.Wu[d], L.Zhang[d], C.F.Dong[e] and Z.Y.Cui[e]

[a]National Institute for Fusion Science, Toki 509-5292, Gifu, Japan
[b]Department of Fusion Science, Graduate University for Advanced Studies, Toki 509-5292, Gifu, Japan
[c]Department of Mechanical Engineering and Science, Kyoto University, Kyoto 606-8501, Japan
[d]Institute of Plasma Physics, Hefei 230031, China
[e]Southwestern Institute of Physics, Chengdu 610041, China

E-mail address: morita@nifs.ac.jp

IAEA Technical Meeting on Atomic, Molecular and Plasma Material Interaction Data for Fusion Science and Technology
Daejeon Convention Center (DCC), Daejeon, Korea
15 - 19 December 2014

This work was partially supported by the LHD project (NIFS14ULPP010), JSPS KAKENHI Grant Number 23340183 and the JSPS-NRF-NSFC A3 Foresight Program in the field of Plasma Physics (NSFC: No.11261140328, NRF: No. 2012K2A6000443).

Contents

Introduction (I): Requirement for W diagnostics and transport study in ITER

- **The following requirement can be solved in LHD.**

1. W diagnostics
- **Line identification**
  - **Visible: divertor plasma (e.g., W^0-W^{2+})**
  - **VUV: SOL plasma (e.g., W^{3+}-W^{6+})**
  - **EUV: edge plasma (e.g., W^{19+}-W^{45+})**
  - **X-ray: core plasma (e.g., W^{65+}-$^{71+}$)** **(not possible in LHD)**
- **Density measurement**
  - **Visible: sputtering at divertor plates**
  - **VUV: influx at SOL**
  - **EUV: W density at plasma edge**
  - **X-ray: W density at plasma core** **(not possible in LHD)**

2. W transport study
- **Calculation of accurate ionization equilibrium**
  - **Ionization and recombination coefficients**

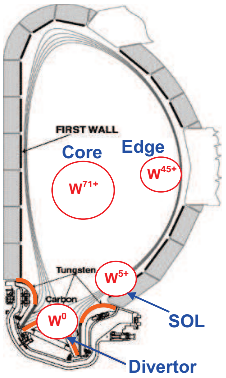

Introduction (II): Max. charge state of W

- LHD
  - NBI (neutral beam injection): T_e<4keV (max. q: W^{46+})
  - ECH (electron cyclotron heating) T_e<20keV
- ITER (max. q: W^{64+} - W^{72+})
  - T_e~T_i~10-20keV at n_e~10^{14}cm^{-3}
  (Observation of W^{72+} & W^{73+} lines is difficult)

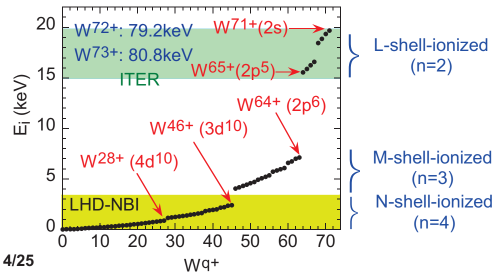

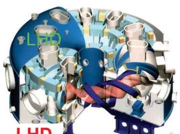
LHD

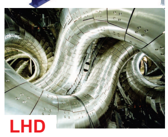
LHD

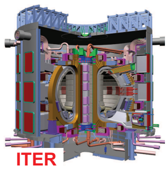
ITER

LHD can accept W pellet injection

- Thin W wire in cylindrical carbon or plastic
- W size: 0.03 - 0.2mm$^{\phi}$ in diameter
- W weight: 9.55x10^{-6}g - 4.25x10^{-4}g
- W particles (N_W): 3.13x10^{16} - 1.39x10^{18} /pellet
- W average density (N_W/V_p): 1.04x10^{9} - 4.64x10^{10} cm^{-3}
  (V_p: LHD plasma volume, N_c/V_p=0.6x10^{13}cm^{-3})

Remarkable benefit of LHD for W spectroscopy:
- Discharge can self-recover, even if T_e is close to zero.
- LHD can produce the brightest W light source.
- W spectra can be measured at a variety of T_e.

W in plastic (hydrocarbon)

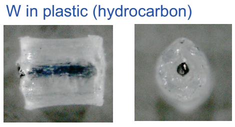

W in graphite carbon

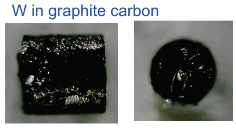

0.7mm

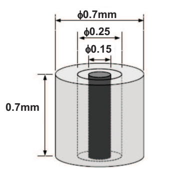

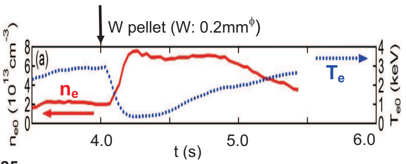

W ion behavior after W pellet injection

- After W pellet injection, higher ionization stages of W ions appear as a function of time.

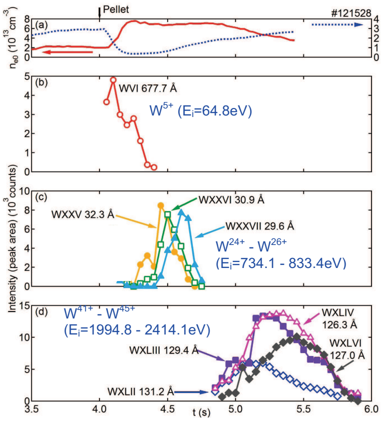

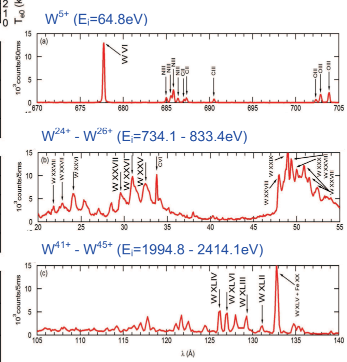

W EUV spectra from LHD in 40-140Å

- W spectra observed with 1200g/mm EUV spectrometer (50-500Å).

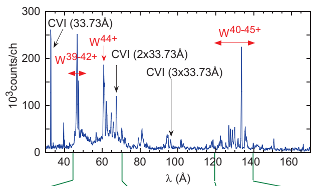

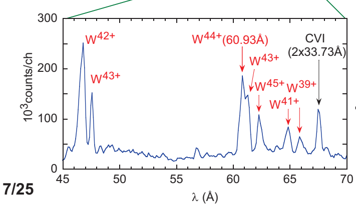

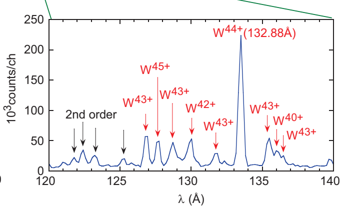

W EUV spectra from LHD in 10-70Å

- W spectra observed with 2400g/mm EUV spectrometer (10-100Å).

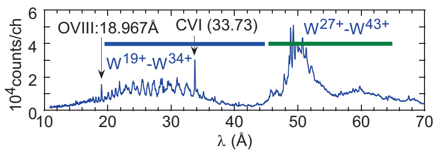

- W^{12+} (E_i=0.258keV) 4s^{2}4p^{6}4d^{10}4f^{14}5s^2 → Not simple configuration
- W^{15+} (E_i=0.362keV) 4s^{2}4p^{6}4d^{10}4f^{11}5s^2
- W^{17+} (E_i=0.421keV) 4s^{2}4p^{6}4d^{10}4f^{11}
- W^{19+} (E_i=0.503keV) 4s^{2}4p^{6}4d^{10}4f^9 → 6g-4f (20-40Å), 5g-4f (20-45Å)
- W^{28+} (E_i=1.132keV) 4s^{2}4p^{6}4d^{10} → 5f-4d (18-30Å), 5g-4f (20-45Å), 4f-4d (45-65Å)
- W^{38+} (E_i=1.830keV) 4s^{2}4p^6 → 4d-4p (60-70Å)

- W^{44+} (E_i=2.354keV) 4s^2 → 4p-4s (60.93, 132.9Å) →
- W^{45+} (E_i=2.414keV) 4s → 4p-4s (62.336, 126.998Å) →

Simple configuration

W^{27+}-W^{43+} in 45-70Å

- Application to plasma diagnostics seems to be difficult in these transitions.

Higher T_e range
E_i=0.881-2.210keV
4d-4p transition array: W^{27+}-W^{43+}
Spectral lines are visible when 4d electrons are partially ionized (W^{28+}: $4s^2 4p^6 4d^{10}$)

Lower T_e range
E_i=0.503-0.881keV
4f-4d transition array: W^{19+}-W^{27+}

Extreme low T_e range
Pseudo-continuum from 4f-4d transition

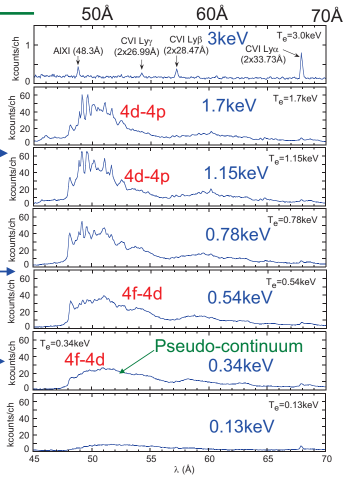

W^{19+}-W^{34+} in 15-45Å

- Electron temperature (T_e) dependence of EUV spectra from LHD.
- Spectral shape changes largely.
- Spectra are composed of W^{19+} to W^{34+} ions ?
- Typical spectrum in 15-35Å is analyzed based on EUV spectra from CoBIT.

CoBIT: Compact EBIT

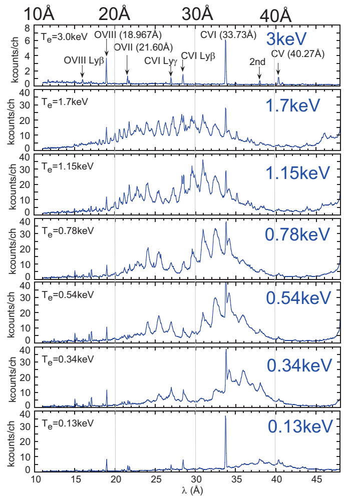

LHD spectrum analysis with CoBIT

- Two CoBIT spectra with different energies of E=950 and 1370eV considered.

CoBIT: Compact EBIT in NIFS

Two CoBIT spectra superposed to simulate LHD spectrum.

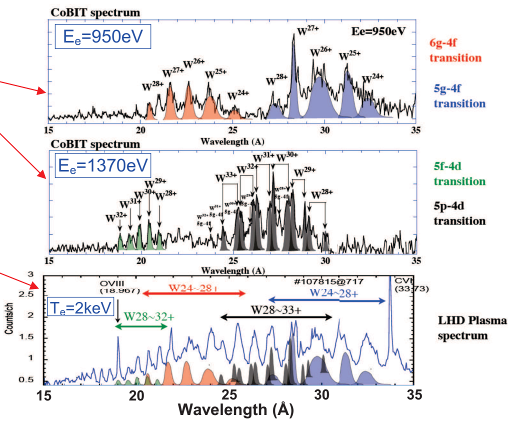

LHD spectrum at 15-35Å composed of
5f-4d of W^{28+}-W^{32+}
6g-4f of W^{24+}-W^{28+}
5p-4d of W^{28+}-W^{33+}
5g-4f of W^{24+}-W^{28+}

Line identification in VUV range (I)

- 3m normal incidence VUV spectrometer
  dλ/dx=0.037Å/pixel = 2.85 Å/mm
  CCD: 13μm/pixel × 1024pixels

W pellet: @4.3s

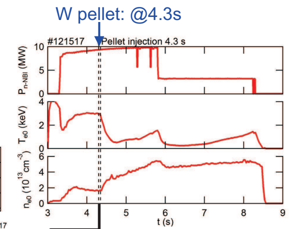

EUV: no W spectrum at just after pellet

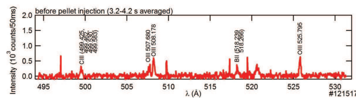

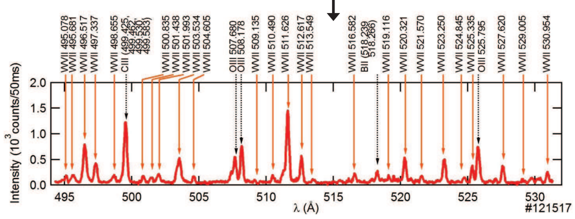

Line identification in VUV range (II) 495-600Å

- Our identification agrees with NIFS database within 0.1Å.
- WVII (W^{6+}) is dominant in this wavelength range.

Results will be soon submitted to Physica Scripta by T.Oishi et al.,

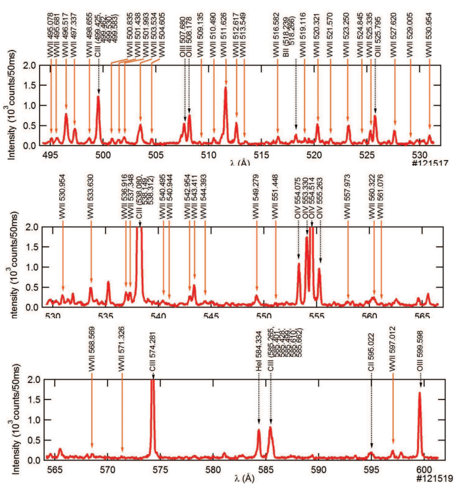

Line identification in VUV range (III) 600-705Å

- WVI (W^{5+}) is bright;

Wavelength (Å)	Counts/50ms
605.926 (5d-6p)	2096.3
605.926 × 2	3080.7
605.926 × 3	1370.0
639.683 (5d-6p)	16535.2
639.683 × 2	8417.0
639.683 × 3	3731.5
677.722 (5d-6p)	13414.8
677.722 × 2	7604.9
677.722 × 3	2117.2
1168.151 (6s-6p)	3449.4

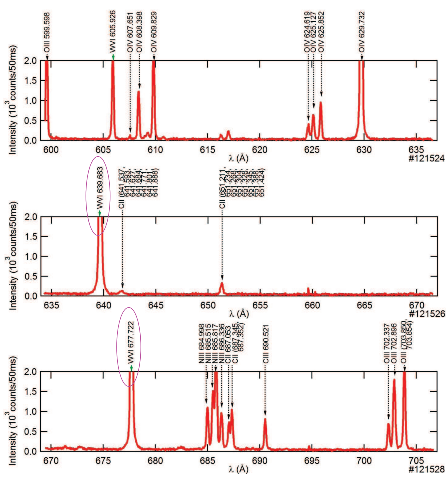

Line identification in VUV range (IV) 705-810Å

- WV (W^{4+}) is dominant in this wavelength range.

- 810<λ≤2200Å
  WV (W^{4+})
  WIV (W^{3+})
  WIII (W^{2+})
  WII (W^{+})
  WI (W^{0})
  are dominantly observed.

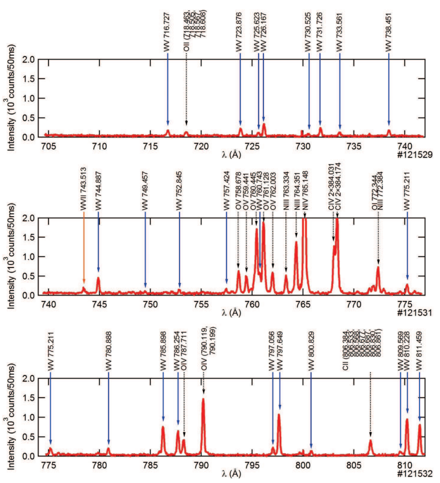

Line identification in Visible range (I)

- W^{26+} M1: $(4f^2)\ ^3H_5$ - $^3H_4$

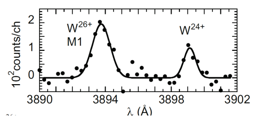

Centrally peaked profile of visible line confirmed M1 transition

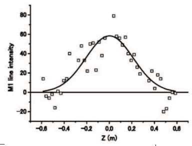

Present results	Previous experiment (EBIT)	Theory
3893.7(4)Å	3894.1(6)Å[a], 3893.5(3)Å[b]	3884.3Å[c] (MCDF)
3899.1(4)Å	Not available	Not available

Polarization also confirmed M1 line: W^{27+} 6693Å?

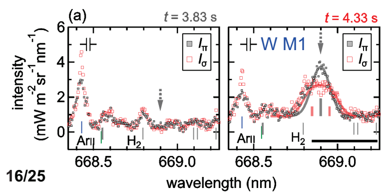

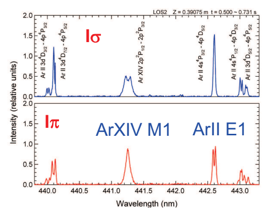

Line identification in Visible range (II)

- W plate inserted into plasma edge boundary

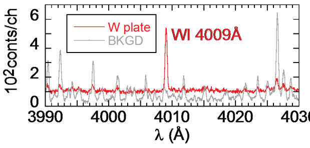

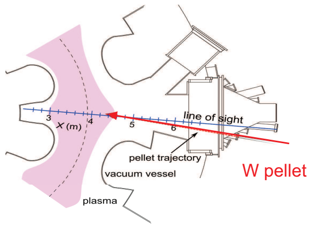

- W pellet ablation cloud directly observed
  - Ablation cloud: T_e=2-3eV, $10^{15} \le n_e \le 10^{17} cm^{-3}$
  - Several lines denoted with arrows are identified by NIST data table
  - WI line at 4009Å is not strong

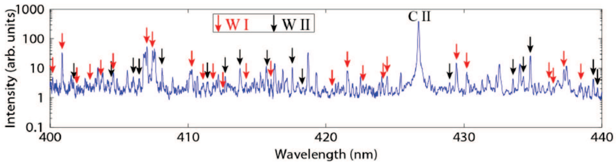

17/25

W (Z=74) density measurement

- Configuration with one or two electrons at outer shell is possible for n_W measurement.

W^{0+}: $1s^22s^2p^63s^23p^63d^{10}4s^24p^64d^{10}4f^{14}5s^25p^64d^6$
W^{6+}: $1s^22s^2p^63s^23p^63d^{10}4s^24p^64d^{10}4f^{14}5s^25p^6$
W^{12+}: $1s^22s^2p^63s^23p^63d^{10}4s^24p^64d^{10}4f^{14}5s^2$
W^{15+}: $1s^22s^2p^63s^23p^63d^{10}4s^24p^64d^{10}4f^{11}5s^2$
W^{17+}: $1s^22s^2p^63s^23p^63d^{10}4s^24p^64d^{10}4f^{11}$
W^{28+}: $1s^22s^2p^63s^23p^63d^{10}4s^24p^64d^{10}$
W^{38+}: $1s^22s^2p^63s^23p^63d^{10}4s^24p^6$
W^{44+}: $1s^22s^2p^63s^23p^63d^{10}4s^2$
W^{45+}: $1s^22s^2p^63s^23p^63d^{10}4s$ — LHD
W^{46+}: $1s^22s^2p^63s^23p^63d^{10}$
W^{56+}: $1s^22s^2p^63s^23p^6$
W^{62+}: $1s^22s^2p^63s^2$ ($3p3s-3s^2$: 79.91Å)
W^{63+}: $1s^22s^2p^63s$ (3p-3s: 77.69Å)
W^{64+}: $1s^22s^2p^6$
W^{70+}: $1s^22s^2$
W^{71+}: $1s^22s$ — ITER
W^{72+}: $1s^2$ ($2p2s-1s^2$: 0.204Å)
W^{73+}: 1s (2p-1s: 0.201Å)

Complicated spectrum needs also complicated modeling for intensity calculation.

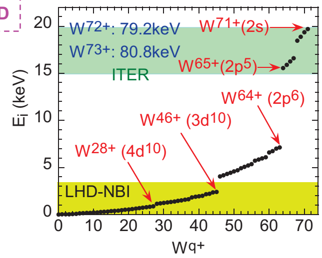

18/25

W^{44+} & W^{45+} with simple configuration

- W^{44+} 4s4p $P_{3/2}$-$4s^2\,{}^1S_0$ (60.93 Å) blended with another line?
  4s4p $P_{1/2}$-$4s^2\,{}^1S_0$ (132.88Å) blended with FeXX (132.85 Å)
- W^{45+} 4p ${}^2P_{3/2}$-4s ${}^2S_{1/2}$ (62.336Å) blended with another line?
  4p ${}^2P_{1/2}$-4s ${}^2S_{1/2}$ (126.998Å) no blend

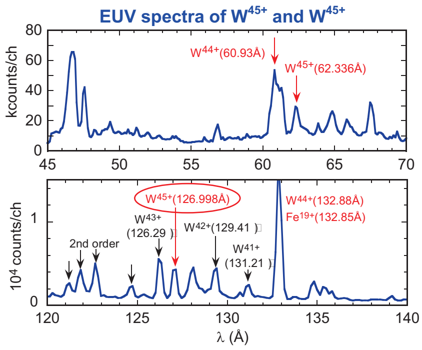

19/25

Density analysis (I): W^{44+} 4s4p-$4s^2$ 60.93Å

- W^{44+} (60.93Å) is blended with another line in low charge state.
- Central W^{44+} density is estimated to be $1.0 \times 10^9 cm^{-3}$.

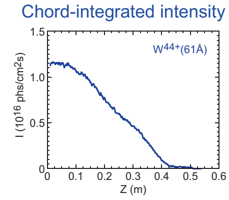

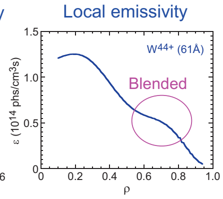

HULLAC with CI: 60.6Å
HULLAC w/o CI: 61.2Å
EBIT, tokamak: 60.87, 60.93Å
LHD: (60.81Å)

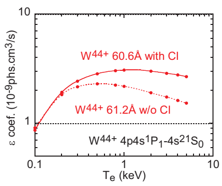

Impurity transport calculation T_e=4.6keV is used.

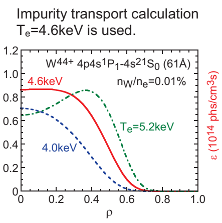

W^{44+} density: $n(W^{44+})/n_e=2.5 \times 10^{-5}$
Total W density: $n_W/n_e=8.8 \times 10^{-4}$

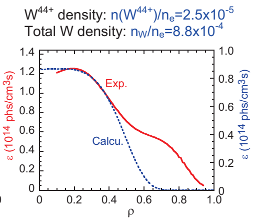

20/25

Density analysis (II): W^{45+} 4p-4s 126.998Å

- Estimated W^{45+} density at plasma center is very similar to W^{44+} density at 60.93Å.

W^{45+} 4p-4s 126.998Å
W^{45+} density: $n(W^{45+})=7.8 \times 10^8 cm^{-3}$
W^{45+} density: $n(W^{45+})/n_e=2.2 \times 10^{-5}$

W^{44+} 4s4p-$4s^2$ 60.93Å
W^{44+} density: $n(W^{44+})=1.0 \times 10^9 cm^{-3}$
W^{44+} density: $n(W^{44+})/n_e=2.5 \times 10^{-5}$

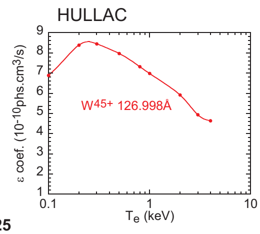

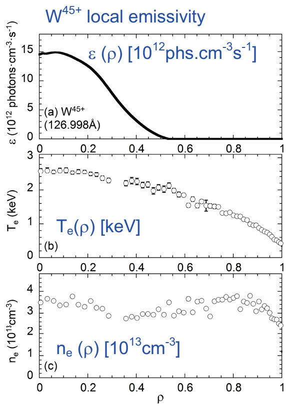

21/25

Ionization & recombination coefficients necessary for impurity transport code

- Local impurity density, n_q, is determined by continuity equation in cylindrical geometry.

$$\frac{\partial n_q}{\partial t} = -\frac{1}{r}\frac{\partial}{\partial r}(r\Gamma_q) - (\alpha_q + \beta_q)n_e n_q + \beta_{q+1} n_e n_{q+1} + \alpha_{q-1} n_e n_{q-1}$$

(α, β : ionization and recombination rate coefficients)

- Radial impurity flux, Γ_q, is expressed by diffusive/convective model;

$$\Gamma_q = -D\frac{\partial n_q}{\partial r} + n_q V$$

(D: diffusion coefficient, V: convective velocity)

- ADPAK original is used in the present study.
  - including a big uncertainty in coefficients.
  - Recombination rate bigger or ionization rate smaller
- Accurate theoretical calculation seems to be difficult.

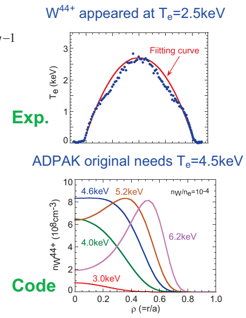

- Estimation of ionization and recombination coefficients from experiments is important.

22/25

Ionization & recombination coefficient evaluation (I)
From radial profiles

- Coefficients can be evaluated from radial profiles of W spectrum and T_e.
- Problems;
- W spectrum blended with other ions.
- Difficulty in Abel inversion.
- Either recombination or ionization is worse?

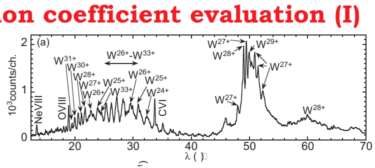

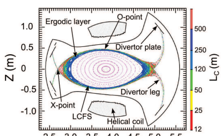

Chord-integrated profile

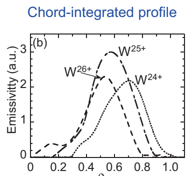

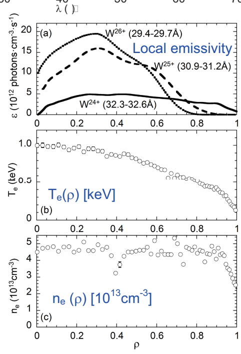

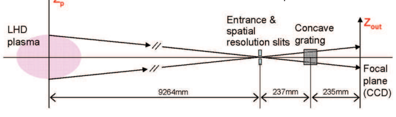

23/25

Ionization & recombination coefficient evaluation (II)
From time behavior during T_e recovery phase

- T_e dependence of W^{44+} is analyzed during T_e recovery phase after W pellet injection.
- Peak intensity of W^{44+} is observed at T_e=2.8keV, whereas the peak abundance of W^{44+} is predicted at T_e=4.5keV by the impurity transport code calculation.

Coefficients can be evaluated from difference between observation and calculation.
But the difference is an integrated effect from W^+ to W^{44+} ions. How we can solve this?

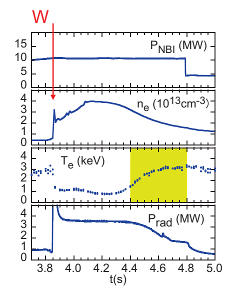

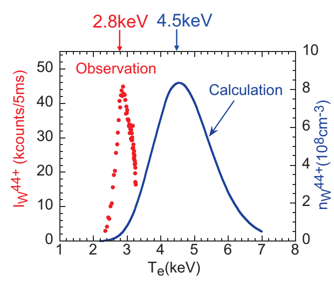

24/25

Summary

- The brightest W light source can be given by LHD plasmas with W pellet injection.
- W spectra have been successfully observed in EUV, VUV and visible ranges.
  (10≤EUV≤600Å, 300≤VUV≤3000 Å, 2500≤Visible≤7000 Å)

  - EUV spectra identified for W^{19+} - W^{45+} ions
  - UTA spectrum at 15-35Å is well analyzed with CoBIT spectra.
  - W^{5+} VUV line found as a new tool for W influx measurement
  - Several WI and WII spectra identified and compared with NIST data.
  - Several M1 transitions found in visible and VUV ranges, e.g. W^{26+} 3893.7 Å.

- W density measurement is attempted for Zn-like W^{44+} and Cu-like W^{45+} ions.
- W^{44+} density is reasonably obtained as $n(W^{44+})/n_e=1.4\times10^{-4}$.
- W^{44+} and W^{45+} are applicable to W density measurement.

Theoretician's work

- Experimental evaluation of ionization and/or recombination rate coefficients is being attempted with two methods;
  - Radial profile measurement of W ion emissions
  - Temporal behavior of W ion emissions during T_e recovery phase
- Collaboration with our data in LHD highly welcomes.